IEEE Access
Multidisciplinary | Rapid Review | Open Access Journal

Received 7 October 2023, accepted 14 November 2023, date of publication 16 November 2023,
date of current version 27 November 2023.

Digital Object Identifier 10.1109/ACCESS.2023.3333881

RESEARCH ARTICLE

A Compact Antenna With Multiple Stubs for ISM, 5G Sub-6-GHz, and WLAN

AZIMOV UKTAM FAKHRIDDINOVICH[1], MD. ABU SUFIAN[1], (Graduate Student Member, IEEE), WAHAJ ABBAS AWAN[1], NIAMAT HUSSAIN[2], (Member, IEEE), AND NAM KIM[1]

[1]School of Information and Communication Engineering, Chungbuk National University, Cheongju-si 28644, South Korea
[2]Department of Smart Device Engineering, Sejong University, Seoul 05006, South Korea

Corresponding author: Nam Kim (namkim@chungbuk.ac.kr)

This work was supported by the Institute for Information & Communications Technology Promotion (IITP) funded by the Korean Government (MSIP) through the Development of Precision Analysis and Imaging Technology for Biological Radio Waves under Grant 2021-0-00490.

ABSTRACT This article describes the design of a tri-band antenna that operates at 2.45 GHz (ISM band), 3.5 GHz (5G sub-6-GHz band), and 5.8 GHz (WLAN band). The antenna design is inspired by a conventional quarter-wave monopole which is fed using a coplanar waveguide feed. Initially, the radiator is loaded with an inverted L-shaped stub to attain broadband across the band spectrum of 2.4 GHz. Then, a pair of two open-ended stubs are etched to achieve a higher frequency band of 5.8 GHz. Hereafter, another open-ended stub is loaded to the right end of the radiating structure, which results in the generation of the Sub-6 GHz 5G (3.5 GHz) band. Finally, the antenna is optimized using parametric analysis to improve the impedance matching across all bands. The proposed antenna offers a tri-band operational mode having frequency ranges from 2.38–2.51 GHz, 3.44–3.84 GHz, and 5.53–7.23 GHz. The reported gains of the proposed antenna at respective frequencies are 2 dBi, 2.1 dBi, and 2.5 dBi having an omnidirectional stable radiation pattern. The antenna prototype is created on a small $20 \times 16 \times 1.6$ mm^3 board and measured to validate the results. Furthermore, the performance of the antenna is compared with the state-of-the-art works to demonstrate its key advantages over similar designs.

INDEX TERMS Tri-band antenna, ISM band, WLAN band, 5G sub-6-GHz antenna.

I. INTRODUCTION

With the exponential increase in the number of wireless devices, significant progress in improved standards with multiple operating frequencies for wireless communication applications has been made in recent years. Moreover, the merging of numerous wireless systems into a single electronic device has boosted the need for multi-band, low-profile, planar, low-cost, and miniature antennas [1], [2], [3]. The band spectrum allocated for Bluetooth (2.4 GHz), Industrial Scientific and Medical (ISM-2.4 GHz), LTE (Long-Term Evolution), the 5G sub-6 GHz spectrum (3.5 GHz), Wireless Local Area Network (WLAN), and 2.45 GHz and 5.8 GHz Radio Frequency Identification (RFID) channels are all popular frequency bands lying inside the frequency band ranging from 2–7 GHz [4], [5], [6], [7], [8], [9]. The simple remedy to the problem is to devise a wide-band antenna covering the complete band spectrum. However, it results in the covering of unwanted band spectra, causing undesirable interference with these bands [10]. Thus, the multi-band antenna becomes the possible solution to overcome this critical challenge.

Among various types of antennas, including Defected Ground Structure (DGS) based antennas [11], metamaterial-based antennas [12], and multi-layered antennas [13], the printed antennas offer more potential, having the advantages of simple structure along with the compact size and broad bandwidths and multiple resonances [14]. A tri-band antenna having a dual inverted L-shaped radiator loaded with an open-ended stub is presented in [15]. The antenna operates

The associate editor coordinating the review of this manuscript and approving it for publication was Bilal Khawaja.

at 1.9, 3.5, and 5.5 GHz, having a maximum gain of 0.13, 2.12, and 3.55 dBi. In [16], a rectangular-shaped monopole is modified using various slits to achieve triband behavior having resonance around 2.44, 3.5, and 5.5 GHz. The antenna offers limited bandwidth at the lower resonance while the radiation pattern is also distorted at all resonating frequencies. A conventional broadband monopole is converted into a triband antenna using a uniplanar asymmetric coplanar strip (ACS) feeding technique along with a modified F-shaped structure [17].

Another ACS-fed antenna mounted with two Split Ring Resonators (SRR) to achieve three distinctive frequencies of 2.4, 5.2, and 5.8 GHz has a peak gain of 0.94, 1.45, and 2.61 dBi, respectively [18]. Another intriguing paper is [19], in which mirrored L-shaped stubs are loaded with an ACS-fed monopole and then a pair of SRRs are loaded at the rear of the radiator to create a multi-band antenna. However, the combination of stubs and SRR increases complexity, and narrow bands along with low gain, limit its usage for modern wireless systems. On the other hand, a metamaterial-inspired printed antenna has been designed [20]. The introduction of metamaterial structure converts the dual-band antenna into a triband antenna at the cost of structural complexity and narrow bandwidths. Moreover, the reported gain is also lower than 2.2 dBi in all passband regions.

A tri-band folded dipole antenna is designed in [21]. The antenna has the advantages of broad bandwidth and high gain at all resonances; however, its large physical size limits its applications for modern-day compact-size devices. Another high gain antenna is presented in [22], where an asymmetric feeding technique is utilized along with various open-ended stub loading techniques to attain multi-band performance. The reported work has the drawback of poor impedance matching at lower resonance along with narrow bandwidth. A geometrical simple conical flask-shaped printed antenna loaded with a slot and pair of open-ended stubs is designed in [23]. The presence of the slot and stub introduces additional resonances at the higher bands; however, the bandwidth is very narrow, resulting in not covering the complete band spectrum allocated globally for targeted applications. A triband antenna for a USB dongle is proposed in [24], and a meander line structured antenna is designed where every arm of the structure results in the generation of different bands. An antenna offers broadband along with moderate gain values but has the drawback of large dimensions.

It can be deduced from the above discussion that there is still a need for multi-band antennas having a compact size, broad bandwidth, high gain, and a geometrically simple structure. Therefore, a compact-sized tri-band antenna is proposed in this article. The conventional Coplanar Waveguide (CPW)-fed L-shaped stub radiator is further modified using a pair of horizontal stubs to achieve resonance of 2.45 GHz, while a vertical stub is inserted to satisfy the frequency band of 3.5 GHz. The optimization of the antenna results in miniaturization while keeping the structure simple, having broad bandwidth and a high gain of more than 2 dBi in all resonances.

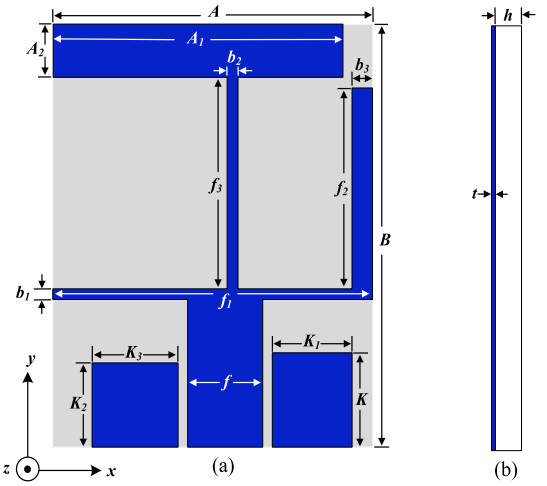

FIGURE 1. Geometry and configuration of the suggested tri-band antenna (a) front and (b) side views.

TABLE 1. The optimized parameters of the proposed tri-band antenna.

Parameter	Dimension	Parameter	Dimension
A	16 mm	K_1	4 mm
A_1	14.5 mm	K_2	4 mm
A_2	2.5 mm	K_3	4.25 mm
f	3.75 mm	b_1	0.5 mm
f_1	16 mm	b_2	0.5 mm
f_2	9.5 mm	b_3	1 mm
f_3	10 mm	t	0.025 mm
K	4.5 mm	h	1.6 mm

II. PROPOSED TRI-BAND ANTENNA DESIGN

This section discusses the proposed tri-band antenna system's structure and process. The working mechanism of the proposed antenna, along with the design steps also explained in this section.

A. CONFIGURATION OF THE PROPOSED TRI-BAND ANTENNA

The layout of the proposed tri-band antenna is exhibited in Fig. 1. The antenna is developed on an FR-4 lossy surface with a dielectric constant εr=4.3, and loss tangent = 0.025. The finalized antenna structure consists of an open stub, a T-shaped strip, a mirrored L-shaped strip, and a coplanar ground plane. The coplanar ground plane is designed on both sides of the feedline with different sizes. The ground plane on the right side has a height and width of K and K_1, respectively.

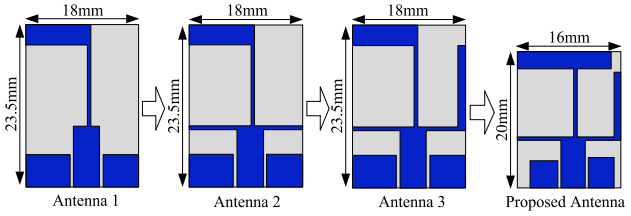

FIGURE 2. Design transformation of the presented tri-band antenna.

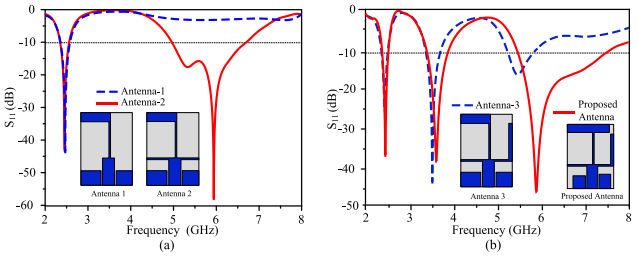

FIGURE 3. $|S_{11}|$ of different antenna design phases (a) antenna-1, and antenna-2 (b) antenna-3, and proposed antenna.

At the same time, the ground plane on the left side has a height of K_2 and a width of K_3. For both simulation and fabricated antenna, standard copper thickness is used as t = 0.035 mm. The antenna is fed by a 50-ohm microstrip feed line, which is connected with a 2.92 mm connector. The suggested antenna system has a small footprint of 20 mm × 16 mm × 1.6 mm^3.

B. ANTENNA DESIGN PROCEDURE

The step-by-step design evolution of the proposed tri-band antenna is illustrated in Fig. 2. The proposed tri-band antenna evolved from the single-band coplanar monopole antenna (Antenna-1). To achieve broadband across the 2.4 GHz band spectrum, the antenna-1 is equipped with an inverted L-shape stub. The radiating patch of antenna 1 offers an operating frequency from 2.38 to 2.51 GHz. To achieve another resonance at 5.8 GHz a horizontal open stub with width and height of f_1 and b_1, respectively, is designed, which can be seen in antenna 2. The S parameter of antenna 2, which also reflect the s parameters of antenna 1 is presented in Fig. 3(a). It can be observed from Fig. 3(a) that the horizontal line provides a wider resonance at 5.8 GHz. In antenna 3, another vertical stub which is situated on the antenna's right side is constructed and optimized and to get resonance at 3.5 GHz. This new stub combined with the horizontal line on the right side offers a resonance at 3.5 GHz. And the left side part of the horizontal radiator gives the resonance at 5.8 GHz. However, the bandwidth is decreased at the upper band for the antenna 3. The s-parameter result of antenna 3 is shown in Fig. 3(b). To reduce the antenna size, the substrate is reduced from the upper part of the positive y-axis, and the patch is extended to the left side, as seen in Fig. 2. In the suggested antenna, the combined effect of the optimized parameter provides a wider resonance at the upper-frequency band. The reflection coefficient of the proposed antenna is illustrated in Fig. 3(b).

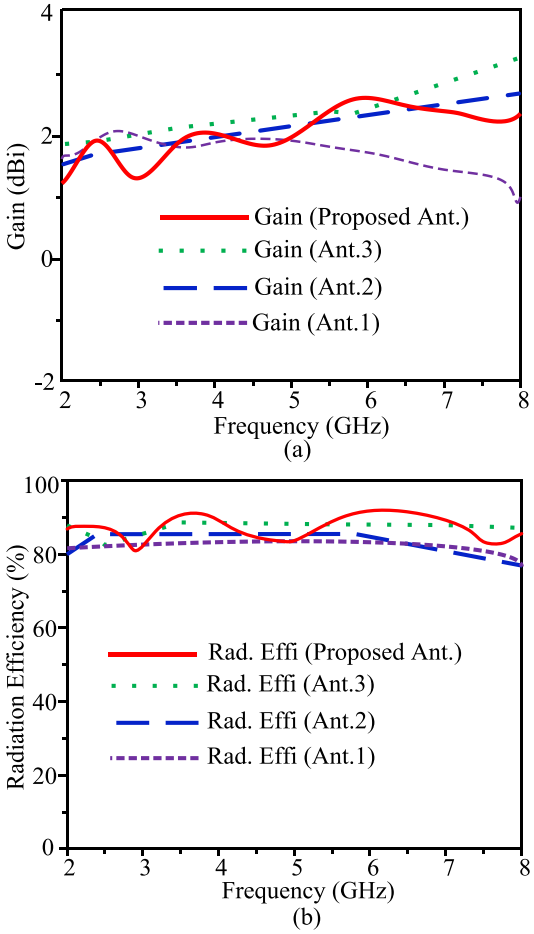

FIGURE 4. Results of the antenna at different design stages (a) gain and (b) radiation performance.

The gain and radiation efficiency of the antenna at different design stages are illustrated in Fig. 4, where Fig. 4(a) represents gain values and Fig. 4(b) shows the radiation efficiency. It can be seen from the results that the suggested antenna has higher gain and radiation characteristics than the initial-stage antenna.

The proposed antenna also has the highest gain characteristics at a higher operating frequency. Overall the proposed antenna offers comparatively high gain and better radiation efficiency while providing a tri-band with a wider operating frequency band than the other antenna stages.

By checking the input impedance, the resonance of any antenna can be realized. At the resonance frequency, ideally, the value of the real part (Rin) of the input impedance should be 50 ohms, while the value of the imaginary part (Xin) should be 0 ohms. The input impedance for the antenna at different design stages is shown in Fig. 5. Input impedance values of all the design stages verify the corresponding stage's resonance which is shown in Fig. 3. In Fig. 5(c), it can be seen that antenna-3's input impedance doesn't match properly at the higher frequency, which results in a poor resonance for the antenna-3 at the higher frequency, and this weak resonance charismatic is observed in Fig. 3(b).

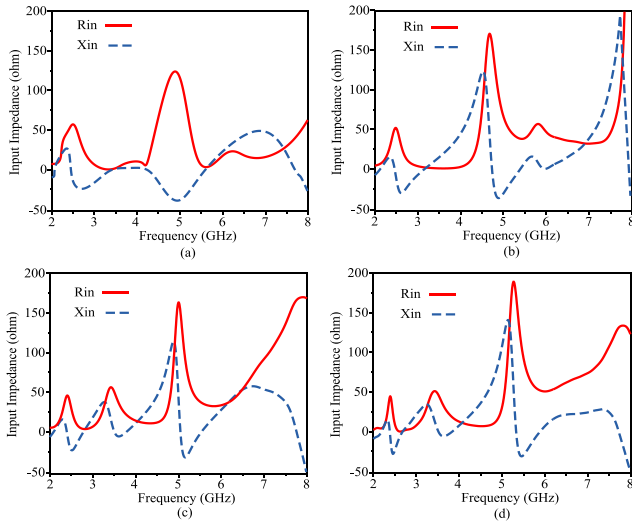

FIGURE 5. Input impedance at different design steps (a) Antenna-1 (b) Antenna-2 (c) Antenna-3 and the proposed tri-band antenna.

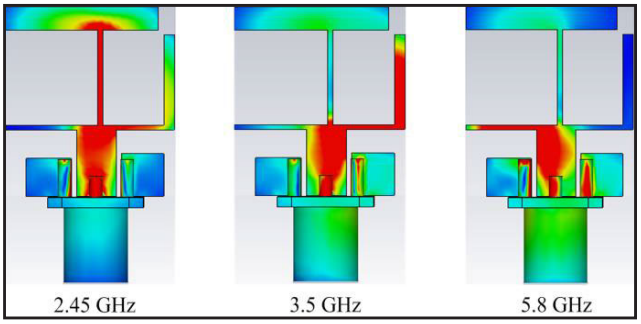

FIGURE 6. The proposed antenna's current distribution at various frequencies.

The current distribution of the finalized antenna for different operating frequencies is depicted in Fig. 6. The current distribution graph verifies the design procedure by representing the active elements for the different frequencies. From the distributed current of the finalized antenna, it is evident that the T-shaped stub works at the 2.4 GHz frequency band (2.38–2.51 GHz), while the open stub combines with the vertical stub of the right-side resonating at the 3.5 GHz frequency band (3.44–3.84 GHz). And the open stub on the left side offers a wider resonance band at 5.8 GHz (5.53–7.23 GHz).

C. PARAMETRIC ANALYSIS

The performance impact on the proposed tri-band antenna is examined in this section by analyzing the length of A_1, f_1, and f_2 of the proposed antenna structure. The results of this investigation are presented in Fig. 7. The optimized values for the proposed antenna are given above in Table 1. This parametric analysis shows the suggested antenna's impedance matching can be altered by changing these parameters, and also the operating frequency band can be shifted based on the requirement by optimizing these parameters.

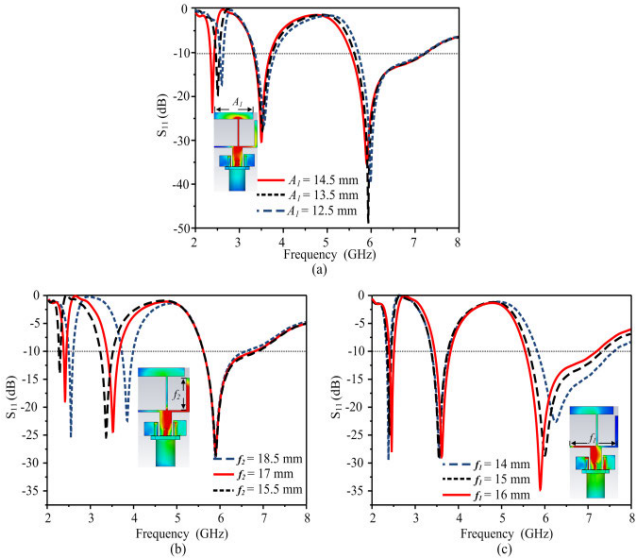

FIGURE 7. Parametric analysis of the proposed tri-band antenna.

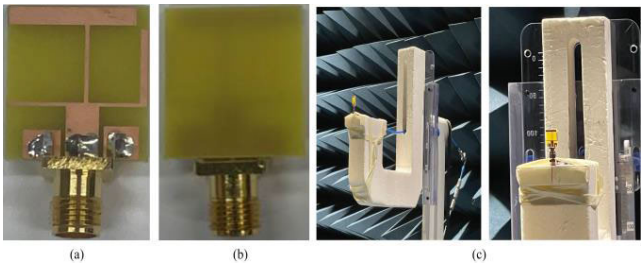

FIGURE 8. Manufactured model and measurement (a) front view, (b) rear view (c) radiation characteristics measurement setup in the anechoic chamber.

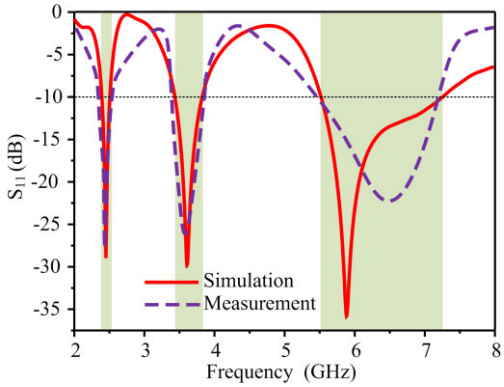

FIGURE 9. S_{11} of the recommended tri-band antenna.

Fig. 7(a) shows the analysis of the parameter A_1 from 12.5 mm to 14.5 mm. The operating frequency of the lower frequency band shifts to the right side by decreasing the value of A_1 and to the left by raising the value of A_1. Similarly, by increasing and decreasing the value of f_2 and f_1, the middle and upper-frequency bands can be changed, respectively, based on the user requirement. Fig. 7(b) illustrates the parametric analysis of f_2 from 15.5 mm to 18.5 mm. At the

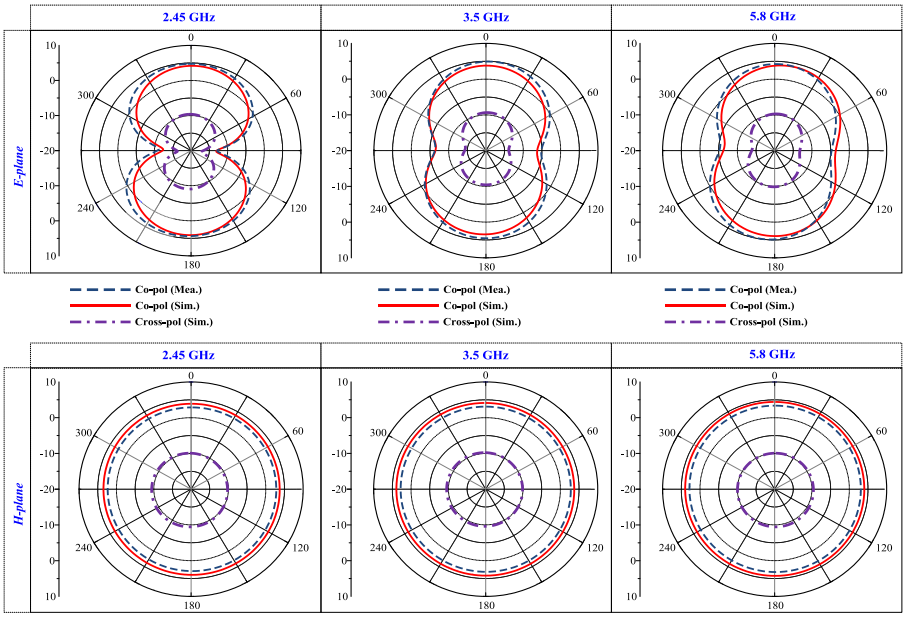

FIGURE 10. Patterns of radiation of the suggested antenna.

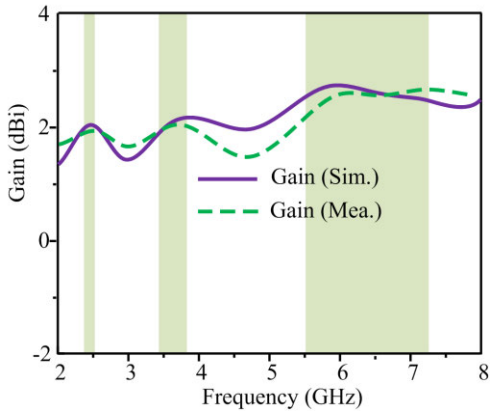

FIGURE 11. Gain versus frequency graph of the proposed work.

same time, the parametric analysis of f_1 from 14 mm to 16 mm is presented in Fig. 7(c). The f_1 is responsible for the tuning of the higher frequency band.

III. RESULTS AND DISCUSSION

A prototype of the proposed tri-band antenna is manufactured and measured to verify the suggested design. Fig. 8(a) and Fig. 8(b) represent the proposed antenna's front view and back view, respectively. At the same time, the radiation characteristics measurement setup in the anechoic chamber is shown in Fig. 8(c). The proposed antenna's results are presented in this section, along with the performance comparison of the proposed antenna with state-of-the-art works.

A. REFLECTION COEFFICIENT

Fig. 9 displays the reflection coefficient (S_{11}) for both simulation and measurement from 2 GHz to 8 GHz. The measurements and the findings of the simulation are in agreement. The matching point for impedance is also suitable, and the antenna resonation is supported in 3 bands. Two lower bands from 2.38–2.51 GHz, and 3.44–3.84 GHz. And an upper band from 5.53–7.23 GHz.

B. RADIATION PATTERNS

The proposed antenna's predicted and measured radiation patterns are examined in both the E- and H-radiating planes at three distinct frequencies which are 2.45 GHz, 3.5 GHz, and 5.8 GHz. The polar plot radiation characteristics of the proposed tri-band antenna are depicted in Fig. 10. The proposed tri-band antenna offers an omnidirectional radiation pattern at all operating frequencies.

C. GAIN AND RADIATION EFFICIENCY

Fig. 11 displays the finalized tri-band antenna's gain characteristics. The antenna provides 2 dBi, 2.1 dBi, and 2.5 dBi gain, respectively, at 2.45 GHz, 3.5 GHz, and 5.8 GHz. It depicts the antenna's stable gain characteristics. The gain is lower at non-radiating bands due to the miss-matching losses, showing the tri-band operation of the antenna.

The simulated and measured radiation efficiency of the proposed tri-band antenna is shown in Fig. 12. The antenna showed a high radiation efficiency of at least 86 % across the operating frequency bands.

The simulated 3D directivity of the antenna at the resonant frequencies is shown in Fig. 13. Directivity and gain patterns are the same for antennas with high radiation efficiency. Since the proposed antenna's radiation efficiency is more than 86%, the directivity plots are similar to the gain radiation curves (shown previously in Fig. 10).

TABLE 2. Performance evaluation in comparison to the published tri-band antennas.

Ref.	Antenna Technique	Dimensions ($\lambda_0 \times \lambda_0 \times \lambda_0$)	Operating Band (GHz)	Peak Gain (dBi)	Radiation Efficiency (%)
[15]	F-shaped planar antenna	0.162 × 0.126 × 0.100	1.89 3.4–3.69 5.15–5.85	0.13 2.12 3.55	83.9
[16]	Slotted printed antenna	0.220 × 0.160 × 0.012	2.4 3.30–3.60 5.15–5.82	1.9 2.1 3	90
[17]	Asymmetric fed uniplanar antenna	0.190 × 0.117 × 0.011	2.2–2.4 3.5–3.7 4.85–6.85	1.7 2.4 3.2	78
[18]	SRRs integrated ACS-fed Monopole	0.251 × 0.094 × 0.012	2.36–2.70 3.35–3.74 5.01–6.12	0.94 1.45 2.61	Not Given
[19]	SRR loaded L-shaped Monopole	0.176 × 0.128 × 0.012	2.4–2.48 5–5.85 8.05–8.50	0.56 1.4 1.9	Not Given
[20]	Metamaterial based monopole	0.187 × 0.173 × 0.011	2.08–2.50 3.42–3.57 5.15–7.28	1.1 1.95 2.17	Not Given
[21]	Folded dipole	0.638 × 0.551 × 0.008	1.53–1.97 2.22–2.56 3.31–4	4.2 4.31 3.02	80
[22]	SRR patch loaded Asymmetric antenna	0.256 × 0.096 × 0.012	2.4–2.74 3.25–3.64	2.7 3.5	Not Given
[23]	CPW-fed monopole antenna	0.311 × 0.233 × 0.012	2.3–2.83 3.34–3.58 5.5–5.9	2.1 2 2.98	76
[24]	planar USB dongle antenna	0.306 × 0.076 × 0.012	2.30–2.69 3.40–3.70 5.15–5.85	2.95	71
Prop. Work	**CPW Monopole**	**0.158 × 0.127 × 0.012**	**2.38–2.51 3.44–3.84 5.53–7.23**	**2 2.1 2.5**	**86**

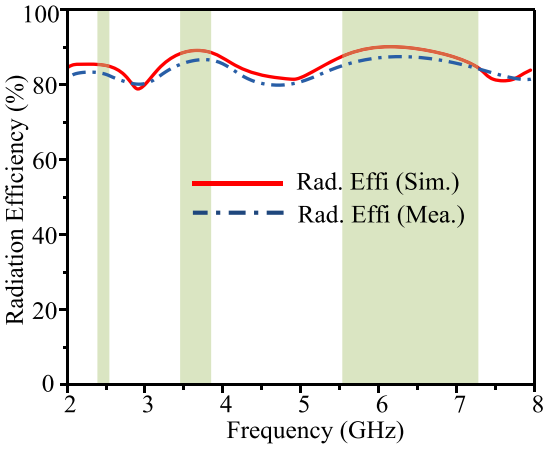

FIGURE 12. Radiation efficiency of the proposed work.

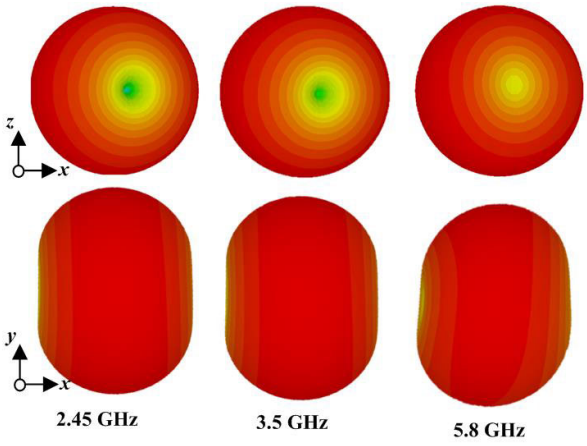

FIGURE 13. Directivity of the proposed tri-band antenna.

D. PERFORMANCE EVALUATION OF THE SUGGESTED ANTENNA WITH SIMILAR TRI-BAND ANTENNAS

The performance of the recommended antenna is evaluated with the tri-band antennas already available from the literature, which are shown in Table 2. The comparison is done based on the antenna's overall dimension, operating frequency band, and peak gain. Some design offers slightly higher gain, especially [21] and [24]. However, those designs

occupy a larger overall volume. The proposed antenna is dominant in terms of size while offering a tri-band characteristic with a comparatively high gain in the operating frequency bands.

IV. CONCLUSION

In this article, a compact tri-band antenna is proposed for ISM, sub-6-GHz, and WLAN applications. The antenna is developed on an FR-4 lossy surface. The antenna is very compact in size ($20 \times 16 \times 1.6$ mm^3). The antenna design is based on a CPW-fed quarter-wavelength monopole. Later, different iterations are made to realize multi-band operation and size reduction. The proposed antenna provides tri-band resonance in three important bands: 2.38–2.51 GHz, 3.44–3.84 GHz, and 5.53–7.23 GHz. The antenna offers an omnidirectional radiation pattern at all operating frequencies while the antenna provides 2 dBi, 2.1 dBi, and 2.5 dBi gain, respectively at 2.45 GHz, 3.5 GHz, and 5.8 GHz. This design also shows more than 86 % radiation efficiency across the operating frequency bands. In summary, the antenna offers a compact size and good radiation performance, which makes it a good candidate for small devices.

REFERENCES

[1] E. H. Lim and K. W. Leung, "Compact multifunctional antennas in microwave wireless systems," in *Compact Multifunctional Antennas for Wireless Systems*, 1st ed. Hoboken, NJ, USA: Wiley, 2012, pp. 1–28.

[2] D. K. Naji, "Miniature slotted semi-circular dual-band antenna for WiMAX and WLAN applications," *J. Electromagn. Eng. Sci.*, vol. 20, no. 2, pp. 115–124, Apr. 2020.

[3] A. J. Abdullah Al-Gburi, Z. Zakaria, M. Palandoken, I. M. Ibrahim, A. A. Althuwayb, S. Ahmad, and S. S. Al-Bawri, "Super compact UWB monopole antenna for small IoT devices," *Comput., Mater. Continua*, vol. 73, no. 2, pp. 2785–2799, 2022.

[4] H. Askari, N. Hussain, D. Choi, M. A. Sufian, A. Abbas, and N. Kim, "An AMC-based circularly polarized antenna for 5G sub-6 GHz communications," *Comput., Mater. Continua*, vol. 69, no. 3, pp. 2997–3013, 2021.

[5] C. Y. Pan, C. H. Huang, and T. S. Horng, "A new printed G-shaped monopole antenna for dual-band WLAN applications," *Microw. Opt. Technol. Lett.*, vol. 45, no. 4, pp. 295–297, 2005.

[6] H. Alwareth, I. M. Ibrahim, Z. Zakaria, A. J. A. Al-Gburi, S. Ahmed, and Z. A. Nasser, "A wideband high-gain microstrip array antenna integrated with frequency-selective surface for sub-6 GHz 5G applications," *Micromachines*, vol. 13, no. 8, p. 1215, Jul. 2022.

[7] S.-H. Lee and Y. Sung, "Multiband antenna for wireless USB dongle applications," *IEEE Antennas Wireless Propag. Lett.*, vol. 10, pp. 25–28, 2011.

[8] N. Hussain, A. Abbas, S.-M. Park, S. Gyoon Park, and N. Kim, "A compact tri-band antenna based on inverted-L stubs for smart devices," *Comput., Mater. Continua*, vol. 70, no. 2, pp. 3321–3331, 2022.

[9] M. Ikram, N. Nguyen-Trong, and A. Abbosh, "Multiband MIMO microwave and millimeter antenna system employing dual-function tapered slot structure," *IEEE Trans. Antennas Propag.*, vol. 67, no. 8, pp. 5705–5710, Aug. 2019.

[10] M. M. Alam, R. Azim, N. M. Sobahi, A. I. Khan, and M. T. Islam, "A dual-band CPW-fed miniature planar antenna for S-, C-, WiMAX, WLAN, UWB, and X-band applications," *Sci. Rep.*, vol. 12, no. 1, pp. 1–16, May 2022.

[11] F. Khajeh-Khalili, A. Shahriari, and F. Haghshenas, "A simple method to simultaneously increase the gain and bandwidth of wearable antennas for application in medical/communications systems," *Int. J. Microw. Wireless Technol.*, vol. 13, no. 4, pp. 374–380, May 2021.

[12] T. Ali, S. Pathan, and R. C. Biradar, "Multiband, frequency reconfigurable, and metamaterial antennas design techniques: Present and future research directions," *Internet Technol. Lett.*, vol. 1, no. 6, pp. 1–7, Nov. 2018.

[13] J. Singh, R. Stephan, and M. A. Hein, "Low-profile penta-band automotive patch antenna using horizontal stacking and corner feeding," *IEEE Access*, vol. 7, pp. 74198–74205, 2019.

[14] N. Hussain and N. Kim, "Integrated microwave and mm-wave MIMO antenna module with 360° pattern diversity for 5G Internet of Things," *IEEE Internet Things J.*, vol. 9, no. 24, pp. 24777–24789, Dec. 2022.

[15] C. V. A. Kumar, B. Paul, and P. Mohanan, "Compact triband dual F-shaped antenna for DCS/WiMAX/WLAN applications," *Prog. Electromagn. Res. Lett.*, vol. 78, pp. 97–104, 2018.

[16] H. Ahmad, W. Zaman, S. Bashir, and M. Rahman, "Compact triband slotted printed monopole antenna for WLAN and WiMAX applications," *Int. J. RF Microw. Comput.-Aided Eng.*, vol. 30, no. 1, pp. 1–8, Jan. 2020.

[17] P. V. Naidu, A. Kumar, and R. Rengasamy, "Uniplanar ACS fed multiband high-gain antenna with extended rectangular strips for portable system applications," *Int. J. RF Microw. Comput.-Aided Eng.*, vol. 29, no. 10, pp. 1–8, Oct. 2019.

[18] L. Kang, H. Wang, X. H. Wang, and X. Shi, "Compact ACS-fed monopole antenna with rectangular SRRs for tri-band operation," *Electron. Lett.*, vol. 50, no. 16, pp. 1112–1114, Jul. 2014.

[19] R. Rajkumar and K. Usha Kiran, "A compact ACS-fed mirrored L-shaped monopole antenna with SRR loaded for multi-band operation," *Prog. Electromagn. Res. C*, vol. 64, pp. 159–167, 2016.

[20] V. Rajeshkumar and S. Raghavan, "A compact metamaterial inspired triple band antenna for reconfigurable WLAN/WiMAX applications," *AEU-Int. J. Electron. Commun.*, vol. 69, no. 1, pp. 274–280, Jan. 2015.

[21] J. Park, M. Jeong, N. Hussain, S. Rhee, P. Kim, and N. Kim, "Design and fabrication of triple-band folded dipole antenna for GPS/DCS/WLAN/WiMAX applications," *Microw. Opt. Technol. Lett.*, vol. 61, no. 5, pp. 1328–1332, May 2019.

[22] K. Kumar Naik, "Asymmetric CPW-fed SRR patch antenna for WLAN/WiMAX applications," *AEU-Int. J. Electron. Commun.*, vol. 93, pp. 103–108, Sep. 2018.

[23] L. Chouti, I. Messaoudene, T. A. Denidni, and A. Benghalia, "Triple-band CPW-fed monopole antenna for WLAN/WiMAX applications," *Prog. Electromagn. Res. Lett.*, vol. 69, pp. 1–7, 2017.

[24] W.-Y. Chiang, C.-H. Ku, C.-A. Chen, L.-Y. Wang, P. A. R. Abu, P.-Z. Rao, C.-K. Liu, C.-H. Liao, and S.-L. Chen, "A power-efficient multiband planar USB dongle antenna for wireless sensor networks," *Sensors*, vol. 19, no. 11, p. 2568, Jun. 2019.

AZIMOV UKTAM FAKHRIDDINOVICH received the B.S. degree in television, radiocommunication, and radio broadcasting from the Tashkent University of Information Technologies, Uzbekistan, in 2013, and the M.S. degree in information and communication engineering from Chungbuk National University, Cheongju-si, South Korea, in 2019, where he is currently pursuing the Ph.D. degree in information and communication engineering. He is also a Research Assistant (RA) with the Optical Information Processing (OIP) Laboratory and Smart Antenna Technologies (SAT). His research interests include antenna design, MIMO systems, metasurface antennas, satellite communication, wireless power transfer, V2X communications, the IoT, EMC, and EMF.

MD. ABU SUFIAN (Graduate Student Member, IEEE) received the B.S. degree in electrical and electronic engineering from American International University-Bangladesh (AIUB), Dhaka, Bangladesh, in 2020. He is currently pursuing the combined M.S. and Ph.D. degrees in information and communication engineering. He is also a Graduate Research Assistant with the Radio Communication Laboratory, Chungbuk National University, South Korea. He is also with the Resonant Wave Technologies Laboratory, Sejong University, South Korea, as a Research Assistant. His research interests include antenna designing for wireless communication, MIMO systems, metasurface antennas, satellite communication, wireless power transfer, V2X communications, the IoT, and BioEM effects of antennas. He is a member of the IEEE Antennas and Propagation Society (IEEE APS), IEEE Microwave Theory and Technology Society (IEEE MTT-S), and IEEE Communications Society (IEEE ComSoc). He is serving as a Reviewer for various journals of multiple publishers, including IEEE, *Nature* (Springer), Wiley, Elsevier, MDPI, EMW Publishing, Hindawi, and Cambridge University Press. He is also serving as a Publication Committee Member for IEEE Smart Cities.

WAHAJ ABBAS AWAN received the B.S. degree in electrical engineering from COMSATS University Islamabad, Sahiwal Campus, Pakistan, in 2019. He is currently pursuing the integrated M.S. and Ph.D. degrees with the Department of Information and Communication Engineering, Chungbuk National University, Cheongju-si, Republic of Korea. He was with the Department of Integrated IT Engineering, Seoul National University of Science and Technology, Seoul, Republic of Korea, from 2019 to 2021. He is also a Research Assistant (RA) with the Optical Information Processing (OIP) Laboratory and Smart Antenna Technologies (SAT) Laboratory under the supervision of Prof. Nam Kim and Dr. Niamat Hussain, respectively. He is the author of more than 50 peer-reviewed conferences and journal articles. He is serving as a Guest Editor for a Special Issue on Recent Advancements in Flexible, Reconfigurable and Wearable Antennas for 5G and Beyond in Micromachine (MDPI) and a Special Issue on Recent Research in Reconfigurable Antenna and Metasurfaces for 5G and Beyond in Electronics (MDPI). He is also serving as a Reviewer for various journals which are not limited to *Micromachine* (MDPI), *Applied Sciences* (MDPI), *Electronics* (MDPI), *International Journal of Microwave and Wireless Technologies*, *International Journal of Antenna and Propagation*, *Radioengineering*, and *Intelligent Automation & Soft Computing* (Autosoft).

NIAMAT HUSSAIN (Member, IEEE) received the B.S. degree in electronic engineering from the Dawood University of Engineering and Technology, Karachi, Pakistan, in 2014, the M.S. degree in electrical and computer engineering from Ajou University, Suwon-si, South Korea, and the Ph.D. degree in information and communication engineering from Chungbuk National University, Cheongju-si, South Korea. Currently, he is an Assistant Professor with the Department of Smart Device Engineering, Sejong University, Seoul, South Korea. His research interests include lens-coupled antennas, metasurface antennas, metamaterial antennas, UWB antennas, mmWave antennas, and terahertz antennas. He was bestowed with the Best Paper Award, in 2017, for his presented paper at the Korea Winter Conference.

NAM KIM received the B.S., M.S., and Ph.D. degrees in electronics engineering from Yonsei University, Seoul, South Korea, in 1981, 1983, and 1988, respectively. He has been a Professor with the School of Information and Communication Engineering, Chungbuk National University, Cheongju-si, South Korea, since 1989. His research interests include optical information processing, the health effect of the EMF, wireless power transfer, and antennas for mobile communications. He is a member of the International Advisory Committee for the World Health Organization Project on EMF, the IEEE International Committee on Electromagnetic Safety, and the International Electro-Technical Commission TC 106. He was the President of the Bio-Electromagnetics Society.